Proc. Estonian Acad. Sci. Phys. Math., 1995, 44, 1, 73–87
https://doi.org/10.3176/phys.math.1995.1.06

ON THE APPLICATION OF THE PSEUDOSPECTRAL METHOD FOR SOLVING THE KORTEWEG–de VRIES EQUATION

Andrus SALUPERE

Tallinna Tehnikaülikool (Tallinn Technical University), Akadeemia tee 1, EE-0026 Tallinn, Eesti (Estonia)

Presented by J. Engelbrecht

Received 9 January 1995, accepted 27 January 1995

Abstract. Several numerical methods have been developed for solving nonlinear evolution equations. In the present paper the application of the pseudospectral method for the numerical integration of the Korteweg–de Vries equation is considered. Advantages of the pseudospectral method, compared with other numerical methods are analysed. Main attention is paid to the accuracy and stability of the method. The behaviour of conserved densities for the first three conservation laws and the influence of the duplication of the number of the grid points on the numerical results are discussed. The corresponding numerical results are presented.

Key words: Korteweg–de Vries equation, numerical integration, pseudospectral method, conservation laws.

1. INTRODUCTION

In the historical perspective the first well-known investigation, where the numerical technique was applied for studying the Korteweg–de Vries (KdV) equation is that by Zabusky and Kruskal [1]. These authors considered the KdV equation

$$u_t + uu_x + \delta^2 u_{xxx} = 0 \tag{1}$$

with the periodic boundary conditions

$$u(x,t) = u(x+Ln), \quad n = \pm 1, \pm 2, \ldots \tag{2}$$

and initial conditions

$$u(x,0) = \cos \pi x \tag{3}$$

($\delta = 0.022$ and $L = 2$). After this pioneering work two main directions have been developed to study the KdV equation:
(i) Gardner et al. [2] found that the KdV equation could be related to the eigenvalue problem of the Schrödinger equation through the inverse scattering method (ISM) developed for quantum mechanics. However, the ISM is mainly used for a special case of an initial excitation which corresponds, in terms of the ISM, to reflectionless potentials and leads to n-soliton solutions. This case is thoroughly investigated by many authors (see for example Drazin and Johnson [3], and Infeld and Rolands [4]).
(ii) For the case of arbitrary initial conditions and particularly for the periodic ones, usually numerical methods are used. Zabusky and Kruskal [1] applied the following finite difference scheme to approximate space and time derivatives

$$u_i^{j+1} = u_i^{j-1} - \frac{\Delta t}{3\Delta x}(u_{i+1}^j + u_i^j + u_{i-1}^j)(u_{i+1}^j - u_{i-1}^j) -$$

$$- \frac{\delta^2 \Delta t}{\Delta x^3}(u_{i+2}^j - 2u_{i+1}^j + 2u_{i-1}^j - u_{i-2}^j), \quad i = 0, 1, \ldots, 2N-1. \tag{4}$$

To raise the accuracy of the finite difference method (FDM), one has to increase the order of the difference scheme, but the computational work, however, grows proportionally with the order of the scheme. That is the reason, why beside the finite difference method (see, for example [5, 6]) several other numerical methods are developed for solving the KdV, modified KdV (MKdV) and KdV-like equations: the Galerkin method [7], the Hopscotch method [8], the Fourier expansion method [9, 10], the split-step Fourier method [11], the spectral methods [9, 12], the pseudospectral methods (PsM) [12–16], etc. See also Dodd et al. [17] for a review of the numerical methods.

The present paper can be considered as the third one in the series. The first [18] was a short report, where a method for detecting the number of emerging solitons from the soliton amplitude curves was presented. In the second paper [19] main attention was paid to the soliton formation process from the spectral viewpoint. The number of emerging solitons was estimated from both the numerical experiment and the ISM. The present work concentrates on the accuracy and stability of the PsM. In Section 2 the problem is stated. Section 3 presents the essence of the PsM, and in Section 4 the accuracy and stability of the method are discussed. Section 5 gives a conclusion.

2. STATEMENT OF THE PROBLEM

Let us consider the KdV equation in the following form

$$u_t + uu_x + du_{xxx} = 0 \tag{5}$$

with the periodic boundary conditions

$$u(x,t) = u(x+2n\pi,t), n = \pm 1, \pm 2, \ldots \tag{6}$$

The initial excitation is given by

$$u(x,0) = -\sin x, \qquad 0 \le x \le 2\pi. \tag{7}$$

The notation

$$d_l = -\log d, \tag{8}$$

where d is the dispersion parameter in (5), is introduced. The problem (5)–(7) is solved numerically (the PsM was applied) for the following values of the parameter d_l:

$$d_l = 0, 0.1, 0.2, \ldots, 1.8, 1.85, \ldots, 2.25, 2.3209. \tag{9}$$

The value $d_l = 2.3209$ corresponds to the value $\delta = 0.022$ used by Zabusky and Kruskal [1] ($d = \pi^2\delta^2$).

3. THE IDEA AND THE ESSENCE OF THE PSEUDOSPECTRAL METHOD

The pseudospectral method was first proposed by Kreiss and Oliger [13]. Let the initial condition $u(x,0)$ be given on the interval 2π. The grid is formed by N points with $\Delta x = 2\pi/N$. The discrete Fourier transform (DFT) is defined by

$$U(\omega,t) = Fu = \sum_{j=0}^{N-1} u(j\Delta x, t) \exp(-2\pi i j\omega/N) \tag{10}$$

and the inverse discrete Fourier transform (IDFT) by

$$u(x,t) = F^{-1}U = \sum_{\omega} U(\omega,t) \exp(2\pi i j\omega/N), \tag{11}$$

where i is the imaginary unit and

$$\omega = 0, \pm 1, \pm 2, \ldots, \pm(N/2-1), -N/2. \tag{12}$$

Here F denotes the Fourier transform and F^{-1} the inverse Fourier transform. Space derivatives are then given by

$$\frac{\partial u}{\partial x} = F^{-1}(i\omega Fu), \tag{13a}$$

$$\frac{\partial^2 u}{\partial x^2} = -F^{-1}(\omega^2 Fu), \tag{13b}$$

$$\frac{\partial^3 u}{\partial x^3} = -F^{-1}(i\omega^3 Fu), \tag{13c}$$

$$\frac{\partial^n u}{\partial x^n} = \mathrm{F}^{-1}\left[(i\omega)^n \mathrm{F}u\right]. \tag{13d}$$

In time, the finite difference leap-frog scheme is used. The KdV equation (5) leads to the following straightforward pseudospectral approximation

$$u(x, t+\Delta t) = u(x, t-\Delta t) - 2\Delta t u \mathrm{F}^{-1}(i\omega \mathrm{F}u) + 2d\Delta t \mathrm{F}^{-1}(i\omega^3 \mathrm{F}u), \tag{14}$$

with the linear stability condition

$$\frac{\Delta t}{\Delta x^3} < \frac{1}{\pi^3}. \tag{15}$$

Fornberg and Whitham [16] proposed to replace $\Delta t\omega^3$ by $\sin\Delta t\omega^3$ in the last term of the expression (14), so the numerical scheme takes the form

$$u(x, t+\Delta t) = u(x, t-\Delta t) - 2\Delta t u \mathrm{F}^{-1}(i\omega \mathrm{F}u) + 2d\mathrm{F}^{-1}\left[i\sin(\Delta t\omega^3)\,\mathrm{F}u\right]. \tag{16}$$

The linear stability condition for scheme (16) is

$$\frac{\Delta t}{\Delta x} < \frac{3}{2\pi^2}. \tag{17}$$

So, the time step which can be used for scheme (16), proposed by Fornberg and Whitham [16], is 4.71 times greater than that of the classical scheme (14). Since $\sin\Delta t\omega^3 = \sin\Delta t\omega^3 + O(\Delta t^3)$, the two methods are identical in the limit Δt decreasing to zero. Scheme (14) is accurate for low enough wave numbers, but if to consider high wave numbers of u, in (14) the dispersive term u_{xxx} dominates over the nonlinear term uu_x and the scheme loses its accuracy [16]. In Fig.1 curve (1) represents the quantity $\Delta t\omega^3$ and (2) represents $\sin\Delta t\omega^3$, the time step Δt corresponds to stability condition (17). These two curves diverge essentially for $|\omega| > 0.25N$ and therefore the influence of higher wave numbers is suppressed for the last term of scheme (16) (see [16] for details). In Fig. 2 there is represented a quantity $(\sin\Delta t\omega^3)/\Delta t\omega^3$, which can be considered as a filter for suppressing the influence of higher harmonics in the last term of expression (14), i.e., applying this filter to scheme (14), one gets in fact scheme (16).

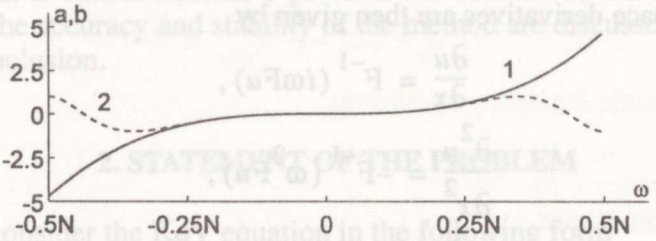

Fig.1. Quantities $a = \Delta t\omega^3$ (1) and $b = \sin\Delta t\omega^3$ (2) against wave numbers ω.

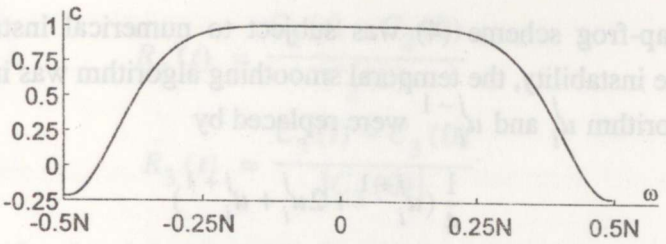

Fig.2. Filter $c = \frac{\sin \Delta t \omega^3}{\Delta t \omega^3}$.

Compared with other numerical methods, the Fourier transform base methods give also additional information in the form of discrete spectra. This information is related to the existence of local minima and maxima in time dependence of spectral curves, the relative values of spectral amplitudes, the concavity and convexity of spectral curves, etc., which present new information about the internal structure of waves [19]. Furthermore, if one needs to filter the data, then the problem is more easily handled by the Fourier method than by the FDM. Besides the PsM, another Fourier method, the spectral method (SM), is widely known. If using the SM to solve a nonlinear equation, one has to apply a convolution operation at each time step. The latter operation, however, takes much more computer time than three fast Fourier transforms (FFT), required at each time step in the case of the PsM. For these reasons the PsM is often used for solving the KdV and related equations (see, for example, [20–25]).

4. ACCURACY AND STABILITY OF THE NUMERICAL SCHEME

Kreiss and Oliger [13] compared the PsM and the FDM, Orszag [12] compared the PsM and the SM. All these authors have found that the PsM is as accurate as other methods, but more effective because it takes less computer time. Fornberg and Whitham [16] also compared the accuracy of the PsM and the FDM. They found that the PsM scheme (16) for 128 points, with stability condition (17), was as accurate as the 8th-order finite difference scheme for 256 points, or the 6th-order finite difference scheme for 512 points, or the 4th-order finite difference scheme for 1024 points.

Taha and Ablowitz [26], and Nouri and Sloan [27] compared different numerical methods. Test problems were one soliton solution and two soliton collisions with different values of the amplitude. All these authors have established that the modified PsM (16) is sufficiently accurate, stable and fast.

The numerical instability in the usage of the finite difference leap-frog scheme for integrating the KdV equation is studied for example by Chan and Kerkhoven [28], He-Ping and Ben-Yu [29], and Aoyagi and Abe [30, 31], who have proposed several methods to extend the stability limits. By Aoyagi and Abe [30], Zabusky, in private communication, recognized

that the leap-frog scheme (4) was subject to numerical instability. To suppress the instability, the temporal smoothing algorithm was introduced. By this algorithm u_i^j and u_i^{j-1} were replaced by

$$\frac{1}{4}(u_i^{j+1} + 2u_i^j + u_i^{j+1})$$

and (18)

$$\frac{1}{4}(u_i^j + 2u_i^{j-1} + u_i^{j-2}),$$

respectively, at some time steps. Aoyagi and Abe have shown that the leap-frog scheme generates computational modes, as well as physical modes in the numerical solution. The physical modes converge to the solution of the original partial differential equation. They demonstrated that the instability comes from computational modes and proposed the Runge-Kutta smoother for the finite difference scheme (4), which was found to give better results than those of (18).

In the present study the PsM (16) proposed by Fornberg and Whitham [16] is used. In order to accelerate the whole procedure, the FFT is applied [32, 33]). For $0 \le d_l \le 2.25$ the number of grid points $N = 128$ for the FFT. It was possible to use the time step Δt corresponding to condition (17) up to the value 1.95 of the parameter d_l, but for $d_l = 2.00$ the scheme became unstable. To get a stable solution, the Runge-Kutta smoother was applied at some time steps, but for scheme (16) the result was not as good as described by Aoyagi and Abe [30, 31] for scheme (4). Neither solution was stable for a longer time period, finally it became unstable. To get a stable solution, the time step Δt, corresponding to the linear stability condition (15) was used for $2.00 \le d_l \le 2.25$. Of course, this takes more computer time. For $d_l = 2.32$ it was required to consider the value $N = 256$ for the FFT in order to get a stable solution. Up to $t = 0.5t_R$ it was possible to use Δt by condition (17), but for $t > 0.5t_R$, the time step corresponding to condition (15) was used (t_R is the recurrence time [1]).

To estimate the accuracy of computations, the first three conservation laws were studied. In the discrete case the quantities

$$C_1(t) = \sum_{i=1}^{N} u(x_i, t), \tag{19}$$

$$C_2(t) = \sum_{i=1}^{N} [u(x_i, t)]^2, \tag{20}$$

$$C_3(t) = \sum_{i=1}^{N} \left\{ \frac{1}{3}[u(x_i, t)]^3 - d[u_x(x_i, t)]^2 \right\} \tag{21}$$

are conserved densities for Eq. (5). In (21) d is the dispersion parameter. Therefore the quantities C_1, C_2, and C_3 must remain constant for this problem. Figures 3 and 4 present the time dependence of relative errors

$$R_2(t) = \frac{C_2(t) - C_2(0)}{C_2(0)} \tag{22}$$

and

$$R_3(t) = \frac{C_3(t) - C_3(0)}{|C_3(0)|} \tag{23}$$

respectively (for d_l = 1.1, 1.9, 2.32). For smaller values of the parameter d_l the relative error R_2 oscillates around a certain zero level (Fig. 3a) and has quite small values (for example order of 10^{-10} for d_l = 1.1). If the parameter d_l increases, one can find that the form of oscillation has changed essentially (Fig. 3b) and the maximal values of the quantity R_2 have also increased by several orders. In Fig. 4a, b such significant changes in the shape of curves cannot be noted as in Fig. 3a, b, only the quantity R_3 has values three orders higher for d_l = 1.9 than for d_l = 1.1. As was mentioned above, for d_l = 2.32 the value N = 256 was used for the FFT. For $t \leq 0.5t_R$ the time step Δt corresponds to condition (17), and for $t > 0.5t_R$ condition (15) was used. The influence of the diminution of the time step at $t = 0.5t_R$ on the relative errors R_2 and R_3 is clearly visible in Figs. 3c and 4c.

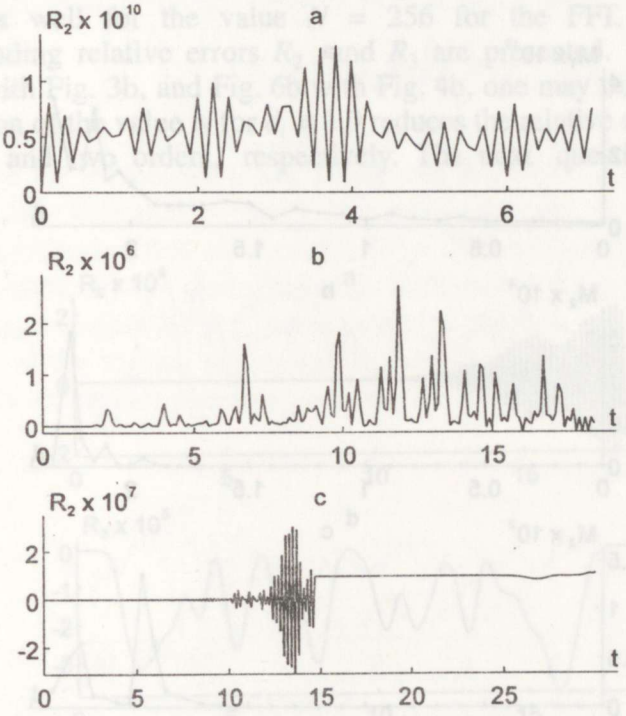

Fig. 3. Time dependence of the relative error R_2 for d_l = 1.1 (a), d_l = 1.9 (b), and d_l = 2.32 (c).

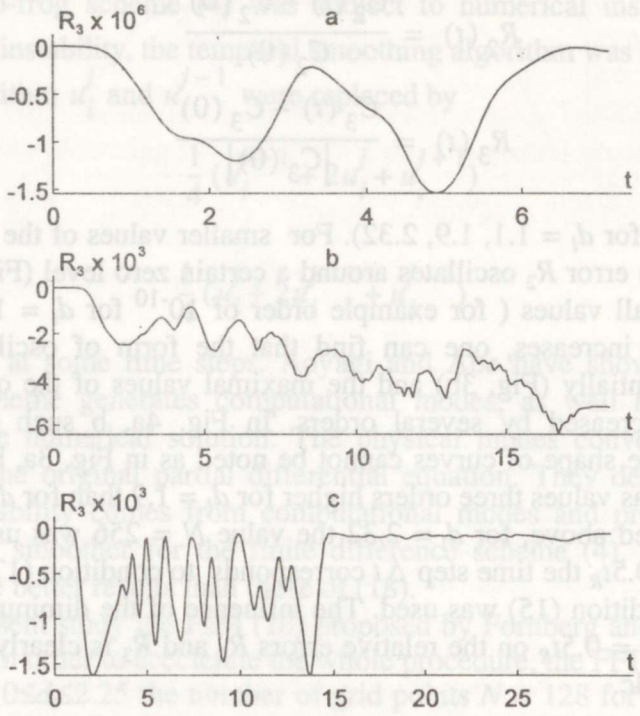

Fig. 4. Time dependence of the relative error R_3 for $d_l = 1.1$ (a), $d_l = 1.9$ (b), and $d_l = 2.32$ (c).

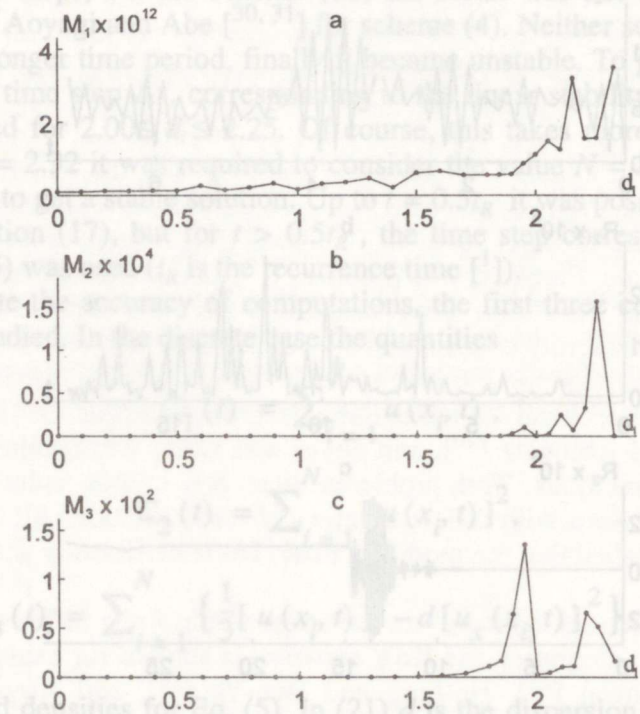

Fig. 5. Maximal deviation M_1 for the conserved density C_1 (a) and maximal relative errors M_2 and M_3 for the quantities C_2 (b) and C_3 (c) depending on the dispersion parameter d_l.

Figure 5a presents the maximal deviation for the quantity C_1 against the parameter d_l

$$M_1(d_l) = \max_t C_1(t, d_l); \tag{24}$$

in Fig. 5b the maximal relative error for C_2 depends on d_l

$$M_2(d_l) = \max_t R_2(t, d_l); \tag{25}$$

and Fig. 5c gives those for C_3

$$M_3(d_l) = \max_t R_3(t, d_l) \tag{26}$$

(the time interval $0 \le t \le t_R$ is under consideration).

On the conserved densities C_1, C_2, and C_3 one can make the following conclusions:

(i) The first conservation law is satisfied perfectly, the maximal deviation for quantity C_1 being less than $3.5 \cdot 10^{-12}$ (Fig. 5a).

(ii) For C_2 the relative error R_2 has the maximum value (0.0155%) at $d_l = 2.25$ (Fig. 5b).

(iii) The third conserved density C_3 deviates maximally (1.35%) at $d_l = 1.95$ (Fig. 5c), i.e., just before the scheme was found to be unstable for the condition (17).

In order to understand how the duplication of the number of grid points N influences the numerical results, the problem (5)–(7) for $d_l = 1.9$ was solved as well for the value $N = 256$ for the FFT. In Fig. 6 the corresponding relative errors R_2 and R_3 are presented. If to compare Fig. 6a with Fig. 3b, and Fig. 6b with Fig. 4b, one may conclude that the duplication of the value N for $d_l = 1.9$ reduces the relative errors R_2 and R_3 by three and two orders, respectively. The next question is how the

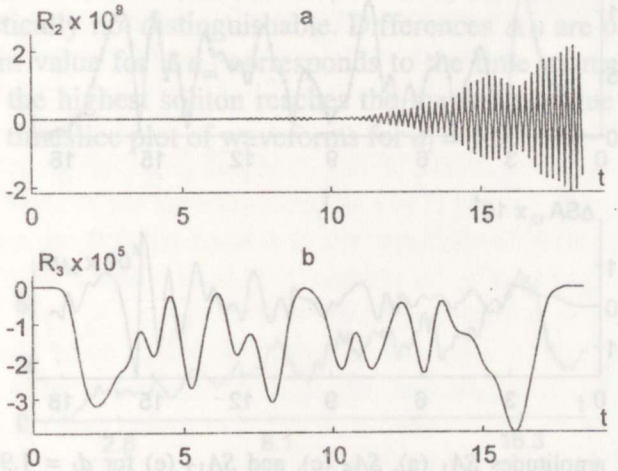

Fig. 6. Relative errors R_2 (a) and R_3 (b) for $d_l = 1.9$ in the case of the value $N = 256$ for the FFT.

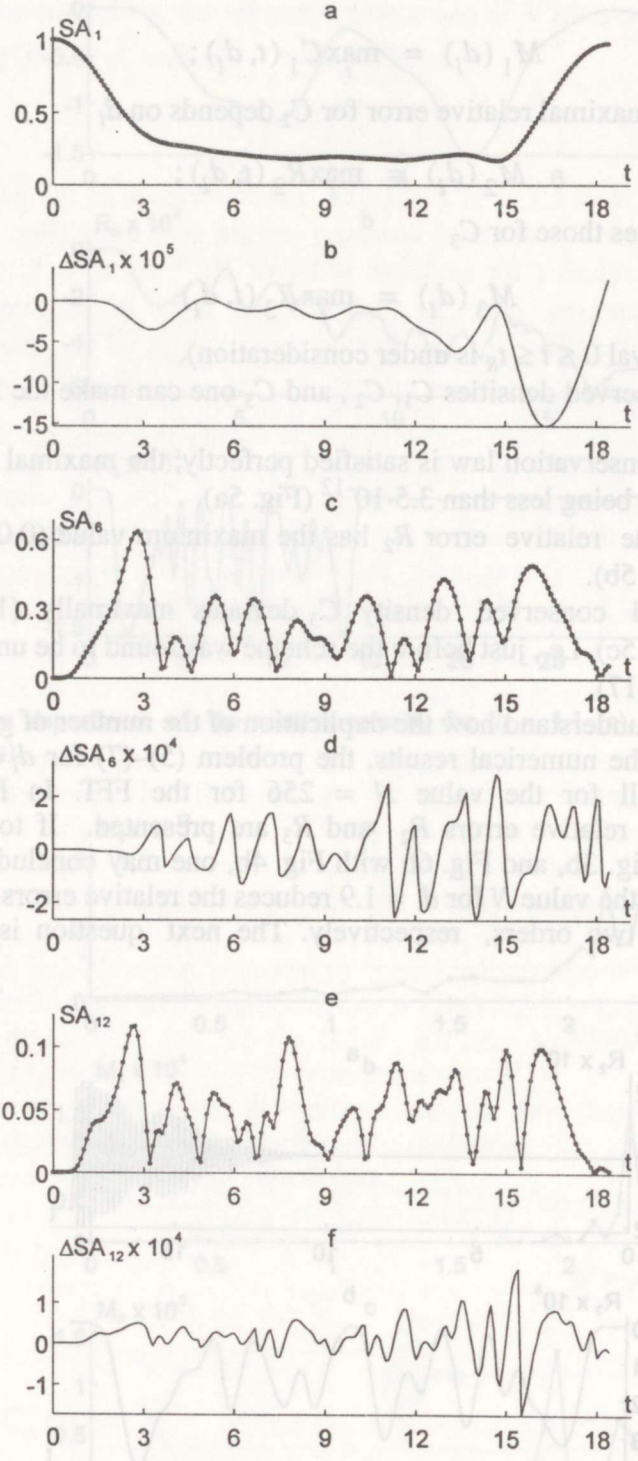

Fig. 7. Spectral amplitudes SA_1 (a), SA_6 (c), and SA_{12} (e) for $d_1 = 1.9$. Solid curves correspond to the value $N = 256$ and dotted curves to $N = 128$. Curves (b), (d), and (f) present the corresponding differences ΔSA_1, ΔSA_6, and ΔSA_{12}.

duplication of the value N influences the spectral characteristics and wave profiles. If the DFT is defined by (10), then the spectral amplitudes can be introduced in the following form:

$$SA_{\omega}(t) = \frac{2|U(\omega, t)|}{N}, \qquad \omega = 1, 2, \ldots, N/2 - 1. \tag{27}$$

Figure 7a, c, e present the spectral amplitudes $SA_{\omega}(t)|_{N=256}$ (solid curve) and $SA_{\omega}(t)|_{N=128}$ (dots) for ω =1, 6 and 12. These solid and dotted curves are practically not distinguishable. In Fig. 7b, d, f the corresponding differences

$$\Delta SA_{\omega}(t) = SA_{\omega}(t)|_{N=128} - SA_{\omega}(t)|_{N=256} \tag{28}$$

are represented. Maximum differences are of order 10^{-4}. To study the differences in the waveforms, the following notation is introduced: space grid

$$x_i = i\Delta x, \quad \Delta x = \frac{2\pi}{256}, \quad i = 1, 2, 3, \ldots, 256; \tag{29}$$

difference between the two waveforms, corresponding to $N = 128$ and $N = 256$,

$$\Delta u(x_i, t) = u(x_i, t)\Big|_{N=128} - u(x_i, t)\Big|_{N=256}, \quad i = 1, 3, 5, \ldots, 255; \tag{30}$$

and the maximum difference between the two waveforms

$$\Delta u_m(t) = \max_{x_i} |\Delta u(x_i, t)| . \tag{31}$$

Figure 8 presents the curve Δu_m against time t. In Fig. 9 there are represented the waveforms u and differences Δu which correspond to the time moments indicated in Fig. 8. One can find again, as well as for the spectral amplitudes, that solid curves (N = 256) and dotted curves (N = 128) are practically not distinguishable. Differences Δu are of order 10^{-3}. The maximum value for Δu_m corresponds to the time moment when the amplitude of the highest soliton reaches the maximum value [34]. Figure 10 presents a timeslice plot of waveforms for $d_l = 1.9$.

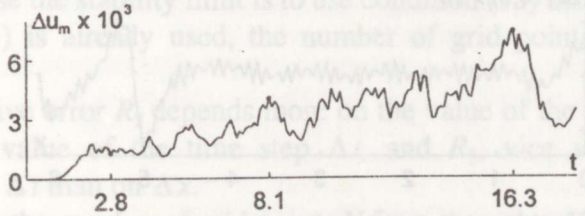

Fig. 8. Maximal differences between waveforms for N=256 and N=128 Δu_m against the time t. Waveforms which correspond to three indicated time moments are presented in Fig. 9.

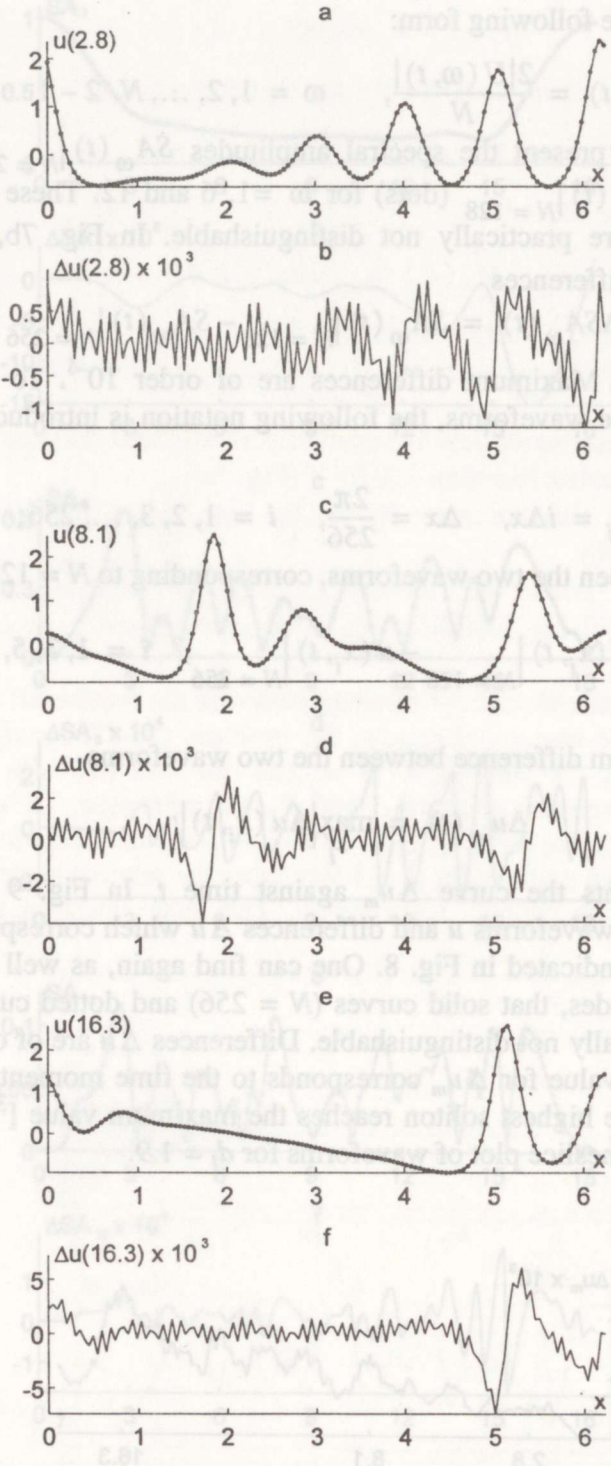

Fig. 9.Waveforms u for $t = 2.8$ (a), $t = 8.1$ (c), $t = 16.3$ (e). Solid curves correspond to the value $N = 256$ and dotted curves to $N = 128$; $d_l = 1.9$. Curves (b), (d), and (f) present the corresponding differences Δu by expression (30).

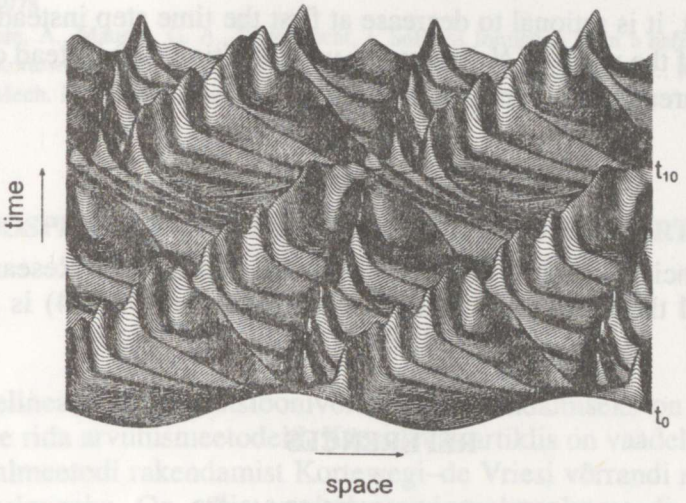

Fig. 10. Timeslice plot for $d_l = 1.9$.

5. CONCLUSION

The pseudospectral method (16) is adequately accurate and stable for solving the KdV equation with the harmonic initial condition. Finally we can make the following conclusions:

(i) If one uses the Fourier transform based methods for the numerical integration of the KdV equation, one gets additional information about the internal structure of waves in the form of discrete spectra, comparing with other methods. In the case of the KdV equation the pseudospectral method is much faster compared with the spectral method, because the PsM does not include the time-consuming convolution operation.

(ii) For solving the problem (5)–(7) it is sufficient to use $N = 128$ for the FFT until the value $d_l = 2.25$.

(iii) If the relative errors R_2 and/or R_3 reach a certain value, scheme (16) becomes unstable. If the stability condition (17) is used, then the simplest way to increase the stability limit is to use condition (15) instead of (17). If condition (15) is already used, the number of grid points N has to be duplicated.

(iv) The relative error R_2 depends more on the value of the space step Δx than on the value of the time step Δt, and R_3, vice versa, is more dependent on Δt than on Δx.

(v) Increasing the number of grid points N from the value 128 to the value 256 decreases the values of conserved densities by several orders, but the corresponding waveforms and spectral densities are practically not

distinguishable. As the computer time for $N = 256$ was 14.9 times larger than for $N = 128$, it is reasonable to use as small values for N as possible, i.e. the value of N for which scheme (16) is still stable. To increase the stability limit, it is rational to decrease at first the time step instead of the duplication of the value of N, i.e., just to use condition (15) instead of (17). The latter increases the computer time 4.7 times.

ACKNOWLEDGEMENTS

The financial support from the French Ministry of Research (in 1993/94) and the Estonian Science Foundation (grant 937/94) is greatly appreciated.

REFERENCES

1. Zabusky, N. J., Kruskal, M. D. Phys. Rev. Lett., 1965, **15**, 240–243.
2. Gardner, C. S., Green, J. M., Kruskal, M. D., Miura, R. M. Phys. Rev. Lett., 1967, **19**, 1095–1097.
3. Drazin, P. G., Johnson, R. S. Solitons: an Introduction. Cambridge University Press, Cambridge, 1989.
4. Infeld, E., Rolands, G. Nonlinear Waves, Solitons and Chaos. Cambridge University Press, Cambridge, 1990.
5. Goda, K. J. Phys. Soc. Japan, 1975, **39**, 229–236.
6. Sanz-Serna, J. M. J. Comput. Phys., 1982, **47**, 199–210.
7. Chin, R. C. Y., Hedstrom, G. W., Karlson, K. E. Math. Comput., 1979, **33**, 647–658.
8. Greig, I. S., Morris, J. L. J. Comput. Phys., 1976, **20**, 64–80.
9. Shamel, H., Elsässer, K. J. Comput. Phys., 1976, **22**, 501–516.
10. Abe, K., Inoue, O. J. Comput. Phys., 1980, **34**, 202–210.
11. Tappert, F. Lect. Appl. Math., 1974, **15**, 215–216.
12. Orszag, S. A. Stud. Appl. Math., 1972, **51**, 253–259.
13. Kreiss, H.-O., Oliger, J. Tellus, 1972, **24**, 199–215.
14. Kreiss, H.-O., Oliger, J. SIAM J. Numer. Anal., 1979, **16**, 421–433.
15. Fornberg, B. J. SIAM J. Numer. Anal., 1975, **12**, 509–528.
16. Fornberg, B., Whitham, G.B. Philos. Trans. Roy. Soc., 1978, **A289**, 373–404.
17. Dodd, R. K., Eilbeck, J. C., Gibbon, J. D., Morris, H. C. Solitons and Nonlinear Wave Equations. Academic Press, London, 1982.
18. Salupere, A., Maugin, G. A., Engelbrecht, J. Phys. Lett., 1994, **A 192**, 5–8.
19. Salupere, A., Maugin, G. A., Engelbrecht, J., Kalda, J. On the KdV soliton formation and discrete spectral analysis (submitted).
20. Peipman, T. Nonlinear Wave Processes in a Medium with Dispersion. PhD Thesis, Tallinn Techn. Univ., Tallinn, 1984 (in Russian).
21. Peipman, T., Engelbrecht, J. Proc. Estonian Acad. Sci. Phys. Math., 1985, **34**, 1, 37–42.
22. Engelbrecht, J., Khamidullin, Y. Phys. Earth Plan. Int., 1988, **50**, 39–45.
23. Newman, W. I., Campell, D. K., Hyman, J. M. Chaos, 1991, **1**, 77–94.
24. Engelbrecht, J., Peipman, T. Wave Motion, 1992, **16**, 173–181.
25. Rosenau, P., Hyman J. M. Phys. Rev. Lett., 1993, **70**, 564–567.
26. Taha, T. R., Ablowitz, M. J. J. Comput. Phys., 1984, **55**, 231–253.
27. Nouri, F. Z., Sloan, D. M. J. Comput. Phys., 1989, **83**, 324–344.
28. Chan, T. F., Kerkhoven, T. SIAM J. Numer. Anal., 1985, **22**, 441–454.
29. He-Ping, M., Ben-Yu, G. J. Comput. Phys., 1986, **65**, 120–137.
30. Aoyagi, A., Abe, K. J. Comput. Phys., 1989, **83**, 447–462.

31. Aoyagi, A., Abe, K. J. Comput. Phys., 1981, **93**, 287–296.
32. Oran Brigham, E. The Fast Fourier Transform and its Applications. Prentice Hall Int., London, 1988.
33. Bracewell, R. N. The Fast Fourier Transform and its Applications. McGraw–Hill, New York, 1978
34. Salupere, A., Maugin, G. A., Engelbrecht, J. Solitons formation from a harmonic input in a Korteweg–de Vries system. Inst. of Cybernetics, Estonian Acad. Sci., Research Report, Mech. 110/94, 1994, (unpublished).

PSEUDOSPEKTRAALMEETODI RAKENDAMISEST KORTEWEGI–de VRIESI VÕRRANDI LAHENDAMISEKS

Andrus SALUPERE

Mittelineaarsete evolutsioonivõrrandite lahendamiseks on välja töötatud terve rida arvutusmeetodeid. Käesolevas artiklis on vaadeldud pseudospektraalmeetodi rakendamist Kortewegi–de Vriesi võrrandi numbriliseks integreerimiseks. On välja toodud pseudospektraalmeetodi eelised võrreldes teiste numbriliste meetoditega. Põhitähelepanu on pööratud vaadeldava meetodi täpsusele ja stabiilsusele. Sel eesmärgil on uuritud, kui täpselt on vaadeldava arvutusprotsessi käigus rahuldatud kolm esimest jäävusseadust ja kuidas mõjutab x–koordinaadi punktide arvu kahekordistamine arvutustulemusi. On esitatud vastavad arvutustulemused.

ПРИЛОЖЕНИЕ ПСЕВДОСПЕКТРАЛЬНОГО МЕТОДА ДЛЯ РЕШЕНИЯ УРАВНЕНИЯ КОРТЕВЕГА–де ВРИЗА

Андрус САЛУПЕРЕ

Для решения нелинейных эволюционных уравнений существует целый ряд численных методов. В настоящей статье рассматривается приложение псевдоспектрального метода для численного интегрирования уравнения Кортевега–де Вриза. Названы преимущества псевдоспектрального метода относительно других численных методов. Основное внимание обращено на точность и стабильность метода. Исследуется точность удовлетворения первых трех законов сохранения и влияние удвоения числа точек по координате x на численные результаты. Представляются соответствующие численные результаты.